

# PSIDIUM GUAJAVA LEAF EXTRACT AS A REDUCING AGENT FOR THE SYNTHESIS, CHARACTERIZATION AND BIO ACTIVITY OF SILVER NANOPARTICLES

Dr. Nyasha Makuve

PhD University of Johannesburg

**Abstract:** The green synthesis of silver nanoparticles (AgNPs) from *Psidium guajava* leaf extracts, characterization and bioactivity is reported. The optimum synthesis conditions were achieved after 2 h at a temperature of 80 °C in 11 mM silver nitrate and 8 mL *Psidium guajava* leaf extract amount. High throughput characterization such as ultraviolet –visible (UV-Vis) spectrophotometer, Fourier transform infrared spectrophotometer (FT-IR), Scanning electron microscopy (SEM), X-ray diffraction (XRD) and energy dispersive X-ray analysis (EDAX) spectrophotometer were used to confirm the synthesized silver nanoparticles. The 20 nm spherical AgNPs were evaluated as antibacterial agents. Antibacterial studies of synthesized determined by disc diffusion susceptibility test. AgNPs were effective against *Staphylococcus aureus* and *Escherichia coli* bacteria with the highest inhibition zone of 20 mm obtained and MIC value of 7 mg/ml against *E. coli* and 11 mg/ml against *S. aureus* obtained.

**Keywords:** green synthesis, silver nanoparticles, antibacterial activity, *Psidium guajava*

## 1. Introduction

Nanoparticles have a vast range of applications in medicine, electronics, biomaterials, catalysis and energy production.<sup>1,2</sup> Nanoparticles are synthesized from transition metals, silicon, carbon (carbon nanotubes, fullerenes) and metal oxides.<sup>3,4</sup> Some nanoparticles occur naturally but of interest are engineered nanoparticles due to their novel physicochemical properties attributable to their size, chemical composition, surface structure, solubility, shape and aggregation.<sup>5</sup> Of interest are silver nanoparticles (AgNPs) which have gained extensive application in antimicrobial materials, anti-inflammatory, thermal conductivity, chemical reactivity, biological labeling, opto-electronics, catalysis systems and probes for in-vivo imaging.<sup>6,7</sup> There are various nanotechnology methods which produce well defined AgNPs however, these methods are quite expensive, require high pressure and temperature thus are potentially dangerous to the environment.<sup>8</sup>

Alternatively, several plants and plant products have been successfully used for efficient and rapid extracellular synthesis of silver and gold nanoparticles.<sup>9,10</sup> Plants contain phytochemicals which act as reducing agents and also the capping of the stabilized synthesized nanoparticles is done by phytochemicals.<sup>11</sup> Leaf extracts of *Coleus aromaticus*, Barbated skull cup herb extract, *Magnolia kobus* and *Diopyros kaki* leaf extracts leaves extract have also been used for nanoparticles synthesis which displayed good antibacterial properties.<sup>12-15</sup> In this study, *Psidium guajava* extract will be explored for the biosynthesis of AgNPs and the antibacterial activity of the AgNPs will be evaluated.

## 2. Methodology

### 2.1 Sample preparation

Fresh *Psidium guajava* leaves were selected and collected from Chipinge district, Manicaland Province, Zimbabwe. Freshly collected leaves of *Psidium guajava* (Figure 1 (a)) were collected from *Psidium guajava* tree (Figure 1 (b)). The leaves were cut into appropriate size (0.25cm x 0.25 cm) and were washed thoroughly with deionized water in a 250 mL wide neck conical flask to remove surface contaminants before being dried at room temperature in the laboratory for 4 weeks. The sample was then crushed into a fine powder using a pestle and mortar.



Figure 1: (a) *Psidium guajava* leaves

(b) *Psidium guajava* tree

### 2.2 Extraction of plant actives

Plant leaf extract was prepared by mixing 40 g milled leaves with 400 mL deionized water in 500 ml of Erlenmeyer flask and boiled in a water bath at 85 °C for 15 min. The resultant crude extract was cooled and filtered with Whatman filter. The filtrate (extract) was kept at 4 °C to be used for the synthesis process and for further studies.

### 2.3 Phytochemical Analysis

#### 2.3.1 Tests for Alkaloids, phenols and flavonoids

*Psidium guajava* (1 mL) extract was treated with 4 drops of Wagner's reagent (Potassium bismuth iodide solution). Formation of an orange brown precipitate was used as an indicator for the presence of alkaloids. To 5 mL of *Psidium guajava* extract few drops of FeCl<sub>3</sub> (5 %) was added. A deep blue black colour was used as an indicator for the presence of phenols. To 5 mL of *Psidium guajava* extract 4 drops of NaOH (2 %) solution was added. Formation of an intense yellow precipitate which turns to colourless on addition of few drops of dilute H<sub>2</sub>SO<sub>4</sub> was used as an indicator for presence of flavonoids.

#### 2.3.2 Test for triterpenoids, steroids and glycosides

*Psidium guajava* extract (5 mL) was treated with 5 mL CHCl<sub>3</sub> with 4 drops of conc.H<sub>2</sub>SO<sub>4</sub> shake and allowed to stand for 10 min. The formation of a yellow coloured lower layer was used as an indicator for the presence of triterpenoids. 5 ml of *Psidium guajava* extract was treated with 3 drops of acetic anhydride, boiled and cooled. Conc.H<sub>2</sub>SO<sub>4</sub> was added from the side of the test tube and showed a brown ring at the junction of two layers and the formation of upper layer was used as an indicator for the presence of steroids. 2 mL of *Psidium guajava* extract was treated with 0.4 mL of glacial acetic acid containing few drops of FeCl<sub>3</sub> and 0.5 mL of concentrated H<sub>2</sub>SO<sub>4</sub> was added by the side of the test tube. A persistent blue colour was used as an indicator for the presence of glycoside.

#### 2.3.3 Test for coumarins, tannins, quinones and saponins

*Psidium guajava* extract (1 mL), an equal volume of 10 % NaOH was added to 2 mL of extract. The formation of a yellow colour was used as an indicator for the presence of coumarins. Drops of lead acetate were added to 3 mL of *Psidium guajava* extract. The formation of a yellow precipitate was used as an indicator for the presence of tannins. Mayer's reagent was added to *Psidium guajava* extract. The formation of a cream precipitate was used as an indicator for the presence of quinones. 10 mL of *Psidium guajava* extract was placed in a test tube and shaken vigorously. The formation of stable foam was used as an indicator for the presence of saponins.

### 2.4 Synthesis of silver nanoparticles

*Psidium guajava* leaf extract (5 ml) was mixed with 90 mL of 1mM aqueous of AgNO<sub>3</sub> and then heat at 80 °C for 15 min. The formation of brown colour signified the synthesis of silver nanoparticles. At different time intervals 1 mL solution of the reaction mixture was taken for UV-Vis analysis in the wavelength range of 300-600 nm to confirm the synthesis of AgNPs. The wavelength of maximum absorbance ( $\lambda_{max}$ ) was determined from the results and it was used for the optimization studies.

### 2.5 Characterization of *Psidium guajava* leaf extract and the synthesized AgNPs

#### 2.5.1 Ultraviolet-visible (UV-Vis) spectra analysis

The reduction of silver ions (Ag<sup>+</sup>) to silver nanoparticles (Ag<sup>0</sup>) was spectrometrically identified by double beam UV-Vis spectrophotometer at different wavelength (300- 600 nm). The graph of wavelength on X-axis and absorbance on Y-axis was plotted.

#### 2.5.2 Scanning Electron Microscope (SEM) and EDAX

The morphology and elemental composition of the synthesized AgNPs was characterized using scanning electron microscopy (SEM) and Energy dispersive X-ray analysis (EDAX). A suspension of AgNPs was made by dissolving the dried AgNPs. The thin films of the sample was prepared on a carbon coated copper grids by just dropping a very small amount of the sample, extra solution was removed using a blotting paper and the grids were allowed to dry by putting it under the mercury lamp for 5 min and the images were recorded. EDX analysis was carried on SEM instrument using the same sample.

#### 2.5.3 FT-IR Analysis

For FT-IR measurements, AgNP powder sample was prepared by centrifuging the synthesized AgNP solution at 10,000 rpm for 15 min. The solid residue layer containing AgNP is redispersed in sterile deionised water for three times to remove unattached biological components to the surface of nanoparticles that are not responsible for bio-functionalization or capping. The pure residue was dried perfectly in an oven overnight at 65 °C and the powder obtained was subjected to FT-IR measurements carried out at a resolution of 4 cm<sup>-1</sup> in KBr pellets. The FT-IR of the pellet was recorded in the wave number range of 4000-450 cm<sup>-1</sup>.

#### 2.5.4 XRD analysis

For the crystallinity studies, films of colloidal AgNP formed were analysed using X-ray diffraction (XRD) study. A film of AgNPs was made by casting the dried AgNPs on a glass slide. The slide was placed on a diffractometer operating at 40 kv (voltage), current of 30 mA and a Cu-K ( $\alpha$ ) radiation of 0.154 nm. The sample was scanned in the 2  $\theta$  range of 30 – 90°.

### 2.7 Bioactivity application

#### 2.7.1 Antimicrobial activity study of *Psidium guajava* and synthesized silver nanoparticles.

Antimicrobial activities of the *Psidium guajava* and synthesized AgNPs were determined using the disc diffusion susceptibility test. Approximately 20 mL of molten and cooled media (Muller Hinton agar) was poured in sterilized petri dishes. The plates were left overnight at room temperature to check for any contamination to appear. The test organisms grew in selected broth for 24 h. A 100 mL broth culture of each test organism was used to prepare lawns. Agar wells of 6 mm diameter were prepared with the help of a sterilized stainless-steel cork borer. Two wells were prepared in the agar plates. The wells will be labeled as A and B. The plates

containing the test organism, *Psidium guajava*, AgNPs and standard drugs were incubated at 37 °C. The plates were examined for evidence of zones of inhibition. The diameter of the zones of inhibition were measured using a meter ruler and the mean value for each organism was recorded and expressed in millimeter

### 2.7.2 MIC values of synthesized silver nanoparticles against *E. coli* (Gram negative bacteria) and *S. aureus* (Gram positive bacteria).

A dilution test was carried out by adding dilutions of an antimicrobial (synthesized AgNPs) to a broth or agar medium (100 µL Mueller–Hinton broth). A standardized inoculum of the test organism (bacteria at a concentration of 10<sup>5</sup> CFU/mL) was then added. The MIC was read after 24 h of incubation at 37°C as the MIC of the tested substance that inhibited the growth of the bacterial strain. Therefore, control bactericidal tests of solutions were performed containing all the reaction components.

### 3. Results and discussion

Phytochemical tests of *Psidium guajava* leaf extract (**Table1**) revealed the presence of alkaloids, phenols, flavonoids, glycoside, triterpenoids, steroids and tannins by positive reaction with the respective test reagent. The phytochemicals with hydroxyl groups such as hydroxylated polyphenolic compounds (flavonoids and tannins) are responsible for the effective reduction of Ag<sup>+</sup> to Ag<sup>0</sup> nanoparticles in solution. Polyphenolic compounds; flavonoids and tannins are antibacterial compounds that can inhibit bacteria growth. These compounds attribute for the bacteria or mold growth inhibition and the killing of bacteria (bactericidal) or fungus (fungicidal) properties of the extract. They are able to do this because they form complexes with extracellular and soluble proteins and bacterial cell walls. Triterpenoids are aromatic and also inhibit bacteria growth. Saponins's glycosides end has been found to have inhibitory effects on gram–positive organisms such as *S.aureus*.

**Table 1: Phytochemical analysis results**

| Phytochemical | Observation                 | Inference             |
|---------------|-----------------------------|-----------------------|
| Alkaloids     | Orange brown precipitate    | Alkaloids present     |
| Phenols       | Deep blue black colour      | Phenols present       |
| Flavonoids    | Intense yellow precipitate  | Flavonoids present    |
| Triterpenoids | Yellow coloured lower layer | Triterpenoids present |
| Steroids      | Brown ring and green colour | Steroids present      |
| Glycosides    | Blue colour                 | Glycosides present    |
| Coumarins     | Brown colour of extract     | Coumarins absent      |
| Tannins       | Yellow precipitate          | Tannins present       |
| Saponins      | Stable foam                 | Saponins present      |
| Quinones      | Brown colour of extract     | Quinones absent       |

The presence of the phytochemicals was further confirmed by FT-IR analysis according to **Figure 2** which shows broad peaks at 3417 cm<sup>-1</sup>, 2920.09 cm<sup>-1</sup> and 1638.21 cm<sup>-1</sup> attributed to the –OH, –C–H and –C=O functional groups.

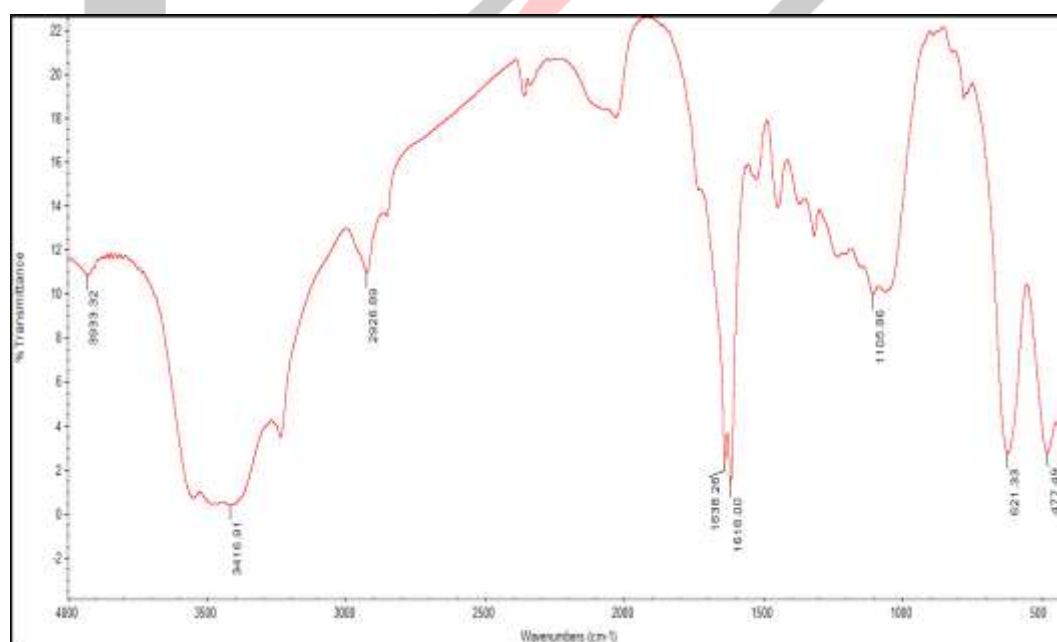


**Figure 2: FT-IR spectra *Psidium guajava* leaf extract**

### 3.1 Characterization of synthesized AgNPs

Immediately after the addition of  $\text{AgNO}_3$  (1mM) aqueous solution to *Psidium guajava* leaf extract, a light yellowish colour was observed which changed to dark brown colour on subjecting to heat (85 °C) for a specified time interval (15 min). This change of colour indicates the formation of AgNP has taken place. With the increased exposure of the reaction mixture to heat (85 °C) the intensity of the colour also increased according to **Figure 3**. AgNPs exhibit a brownish colour in water and this colour arises due to surface Plasmon vibration of metal nanoparticles. Aqueous  $\text{AgNO}_3$  (1 mM) was tested for verification with an exposure to heat (85 °C) and it was found that it did not show any colour change. The colour changes observed agrees very well with literature results.<sup>16</sup>

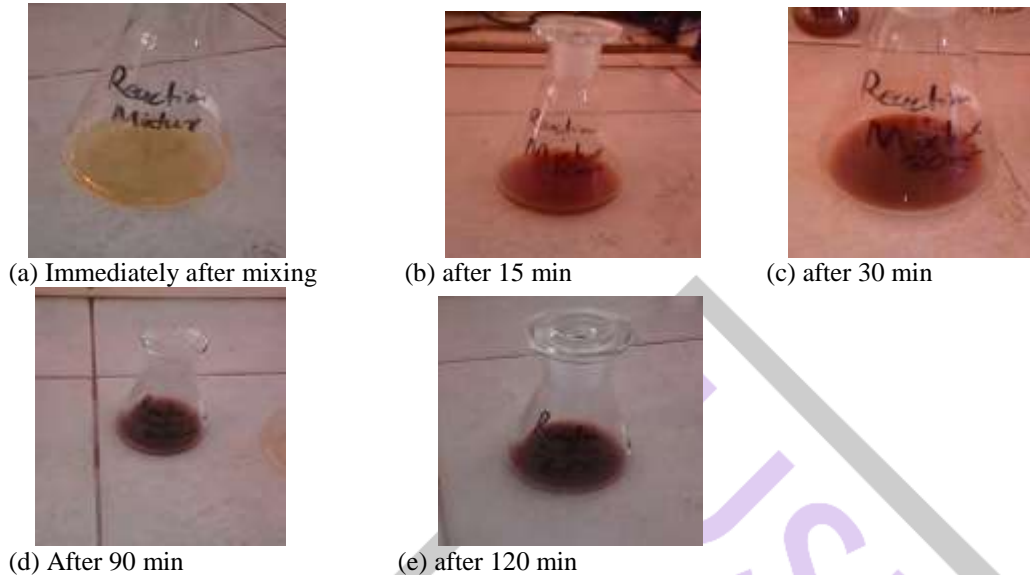


**Figure 3:** Colour changes during AgNPs (a) immediately after mixing (b) 15 min (c) 30 min (d) 90 min and (3) 120 min.

According to **Figure 4** showing the UV-Vis spectrum of the synthesized AgNPs, the region of 380–440 nm has an intense absorption peak as a result of the surface plasmon resonance. Surface plasmon peak observed confirms the influence of aqueous guava leaf extract in reducing  $\text{Ag}^+$  ions to  $\text{Ag}^0$  from aqueous  $\text{AgNO}_3$  solution. The wavelength of maximum absorbance ( $\lambda_{\text{max}}$ ) was determined from the UV-Vis spectra as 420 nm which is the same as the recorded previously by Shanmugam and co-workers.<sup>17</sup>

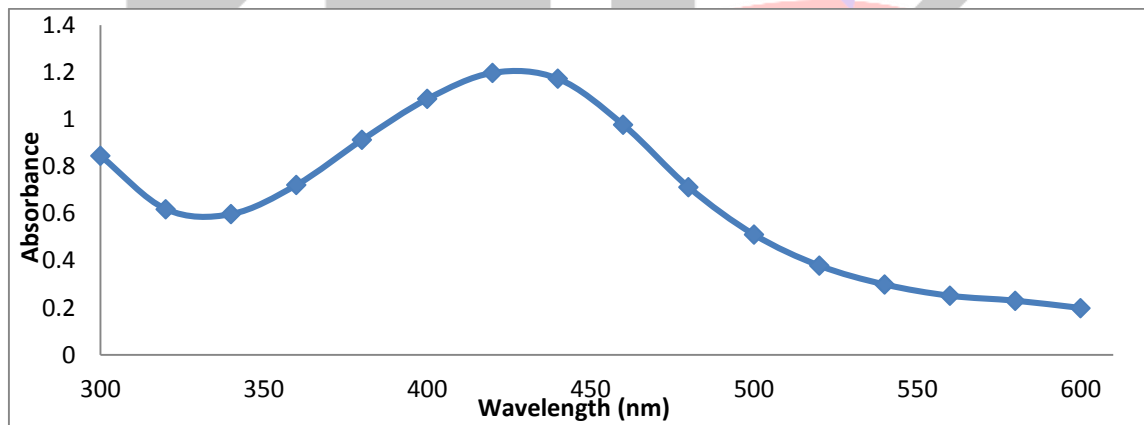


**Figure 4:** UV-Vis spectrum of the synthesized AgNPs

According to **Figure 5** which shows the XRD –spectrum of the AgNPs, the peaks observed at  $2\theta$  values of 38.05, 44.20, 64.50 and 76.39 correspond to Bragg reflections of face- centered (fcc) silver nanoparticles. However the corresponding planes are not shown on the XRD spectrum. This clearly shows that the AgNPs are crystalline in nature. The particle size is responsible for the broadening of peaks in the XRD pattern of solids.



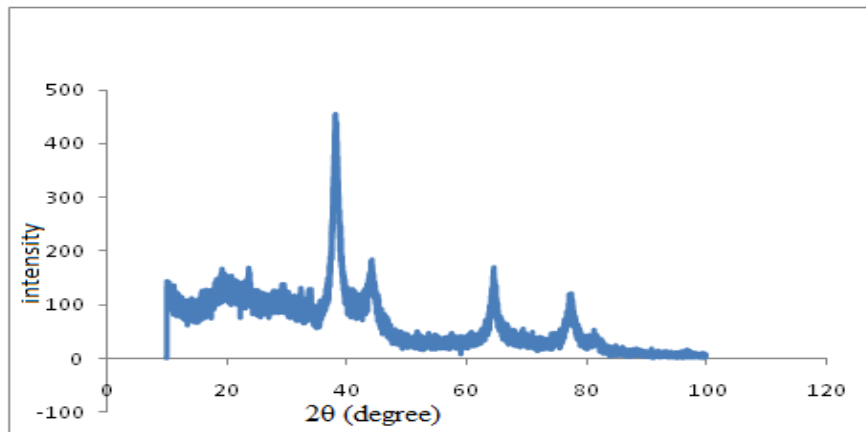


**Figure 5:** XRD pattern of the green synthesised AgNPs

SEM was used to visualize the morphology and size of the AgNPs synthesized. **Figure 6** shows the SEM image of the AgNPs with most nanoparticles spherical in shape with a particle size of 20 nm. This value confirmed the nanosize of the AgNPs synthesized from the leaf extract of *Psidium guajava*.

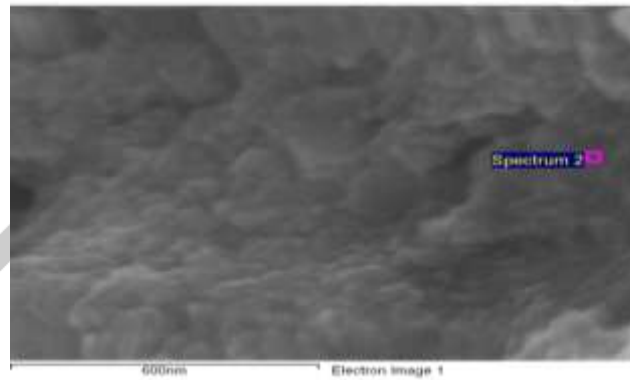


**Figure 6:** SEM micrograph showing synthesized AgNPs

Elemental composition of AgNPs was confirmed by EDAX analysis. According to **Figure 7** there is a strong signal of the Ag atoms which is typical for the absorption of metallic silver nanocrystallites.<sup>18</sup> Other than this peak; there are weaker peaks of carbon and oxygen which may originate from the biomolecules capped on the surface of the AgNPs. Copper peak is as a result of copper grind used during EDAX analysis whereas calcium, magnesium, potassium and aluminum resulted from plant nutrients.

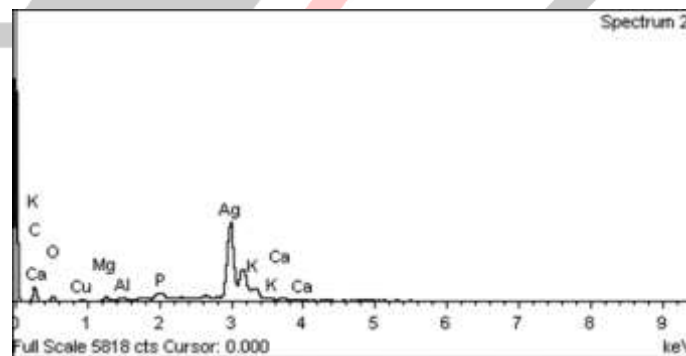


**Figure 7:** EDAX spectra showing the presence of elemental silver in the synthesized AgNPs

### 3.2 Optimization studies

#### 3.2.1 Effect of reaction time

The effect of reaction time was investigated using UV-Vis analysis at different time intervals of the AgNPs reaction mixture. According to **Figure 8**, the surface plasmon resonance was centered on 420 nm which is evidenced by the intense broad peak and as the reaction time increased from 20 min to 120 min; the solution absorbance also increased. Increase in time allows the reaction rate of Ag<sup>+</sup> ions to be reduced as a result there is formation of AgNPs. Absorbance intensity increases steadily as a function of reaction time. After 120 min there was no further increase in absorbance as shown by **Figure 8**. This is because full conversion of Ag<sup>+</sup> ions to AgNPs is done within 120 min.

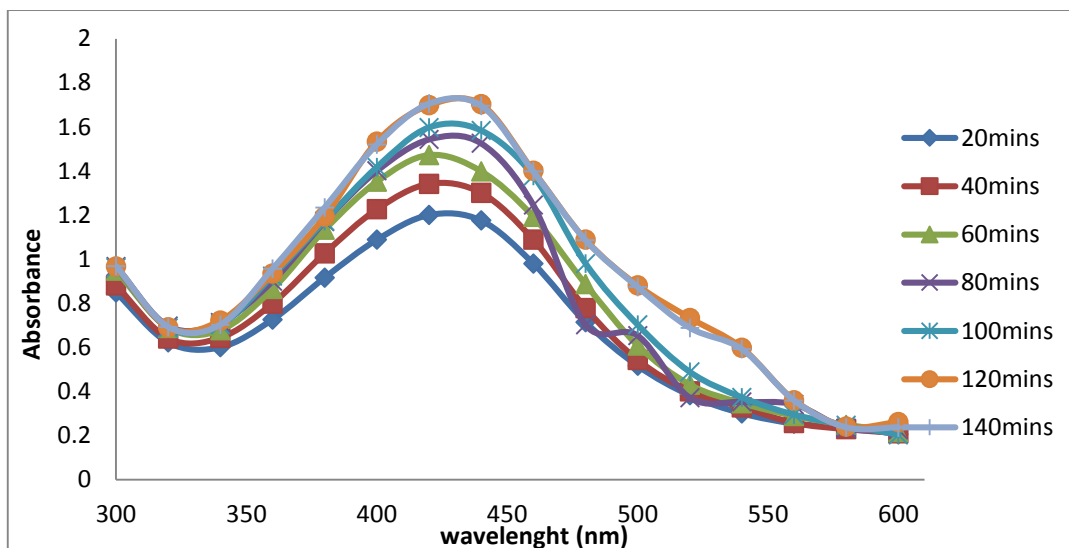


**Figure 8:** Spectra on the effect of reaction time on AgNPs synthesis using 1 mM AgNO<sub>3</sub> and 5 mL *Psidium guajava* leaf extract.

3.2.2 Temperature influence on the synthesis of AgNPs

**Figure 9** shows the graph of the results obtained for the influence of temperature on the reduction of Ag<sup>+</sup> ions in the presence of 5mL *Psidium guajava* leaf extract after 2 h at various temperatures. As the temperature increased from 20 to 80 °C, there was also increase in absorbance from 1.30 to 2.18. Increase in reaction temperature increases the kinetic energy of the reacting molecules hence more Ag<sup>+</sup> ions were being reduced by the extract. However, after 80 °C there is no considerable increase in the absorbance, and this might be the reacting molecules being the limiting factor hence the graph flattens out. The findings are close to the results reported in literature.<sup>19</sup>

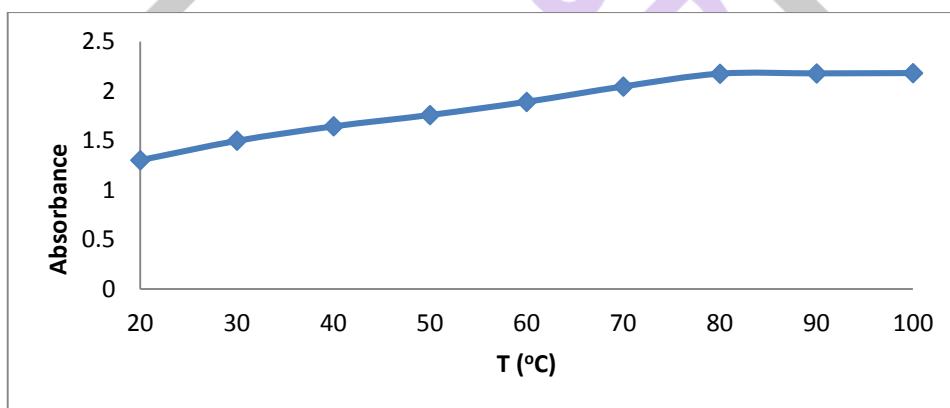


**Figure 9:** Effect of temperature on the synthesis of AgNPs using 1 mM AgNO<sub>3</sub> and 5 mL *Psidium guajava* leaf extract.

3.2.3 Influence of AgNO<sub>3</sub> concentration on the synthesis of AgNPs

The effect of AgNO<sub>3</sub> concentration on the synthesis of AgNPs was carried out by varying AgNO<sub>3</sub> concentration at an absorbance centered at 420 nm for 2 h at a temperature at 80 °C. According to **Figure 10**, as the concentration of AgNO<sub>3</sub> increases from 1 mM to 11 mM the absorbance increases indicating the increase in AgNPs production. Increasing AgNO<sub>3</sub> concentration increases Ag<sup>+</sup> ions in the solution to be reduced by phytochemicals in the *Psidium guajava* leaf extract hence more AgNPs are synthesized. An increase in synthesized AgNPs is presided over by the reduction of Ag<sup>+</sup> to Ag<sup>0</sup>. After 11 mM the optimum metal precursor there was no significant increase in absorbance thus the graph flattens out. This was caused by the limited reducing phytochemicals in the reaction mixture thus no more reduction of Ag<sup>+</sup> to Ag<sup>0</sup>.

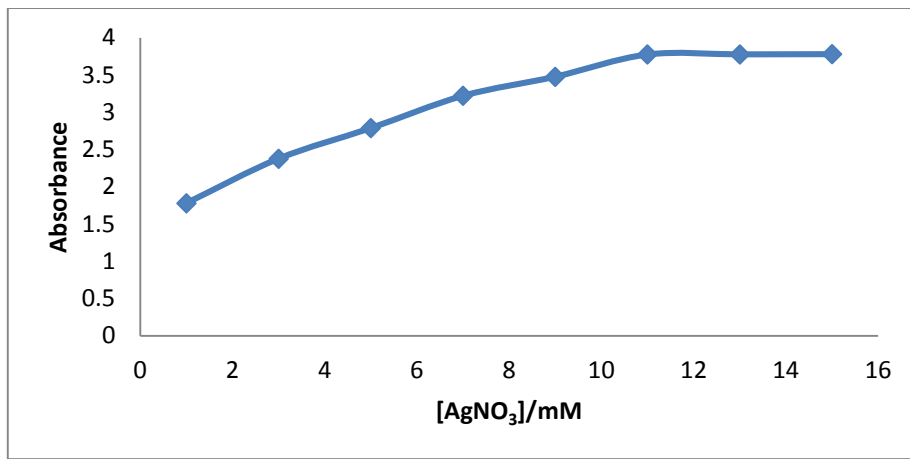


**Figure 10:** Effect of AgNO<sub>3</sub> concentration on the synthesis of AgNPs using 5 mL *Psidium guajava* leaf extract

### 3.2.4 Influence of *Psidium guajava* leaf extract amount on the synthesis of AgNPs

**Figure 11** shows the effect of extract amount on the AgNPs synthesis. As the extract amount increased from 2 – 8 mL; there was considerable increase in AgNPs absorbance which shows increase in AgNP production. The increase in absorbance signals the increased production of AgNPs. The reduction of Ag<sup>+</sup> ions is effective at 8 mL and after that the graph flattens out. Thus, the optimum amount of *Psidium guajava* leaf extract is 8 mL. After 8 mL of the extract amount there is no significant increase in absorbance which means there is no significant increase of produced AgNPs. Above 8 mL it is evocative that the amount of the reducing agents in the extract becomes in excess and the concentration of the silver ions becomes the restraining agent.

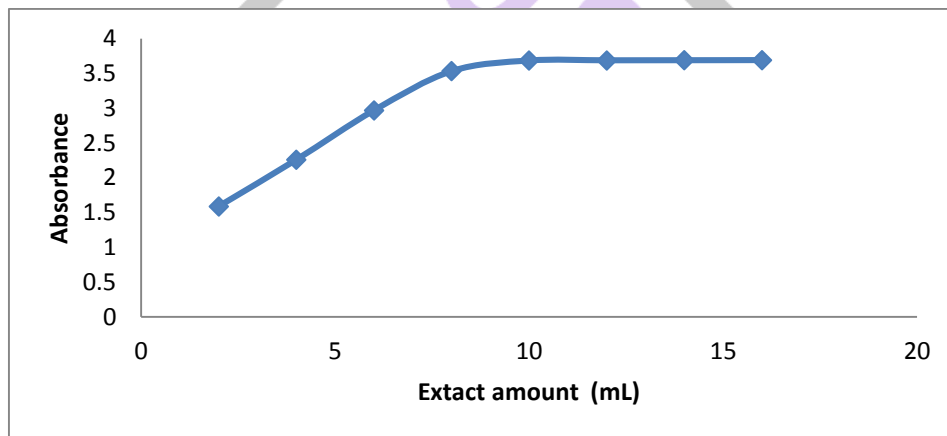


**Figure 11:** *Psidium guajava* Effect of extract amount

### 3.3 Antimicrobial activity

Antibacterial activity of *Psidium guajava* leaf extract and synthesized AgNPs was determined using agar disc diffusion technique against the gram-positive bacterium *Staphylococcus aureus* (*S.aureus*) (**Figure 12**) and gram - negative bacteria *Escherichia coli* (*E.coli*) (**Figure 13**) with bioactivity compared against known drugs such as Gentamicine, Amoxicillin and Cloxacillin. Bacterial inhibition was indicated by a clear zone around the paper discs impregnated with antibiotic substances. The synthesized AgNPs can be an alternative source of antimicrobial as they exhibited strong inhibition against gram positive (*S.aureus*) and gram negative (*E.coli*) bacteria strains.

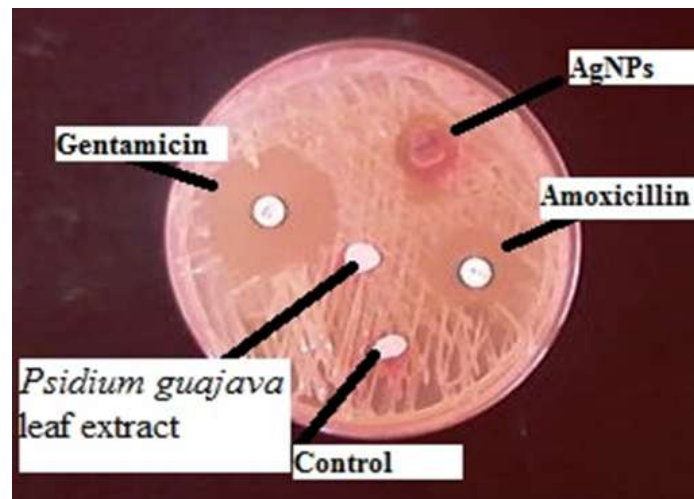


Figure 12: Inhibition zone against (*S.aureus*)

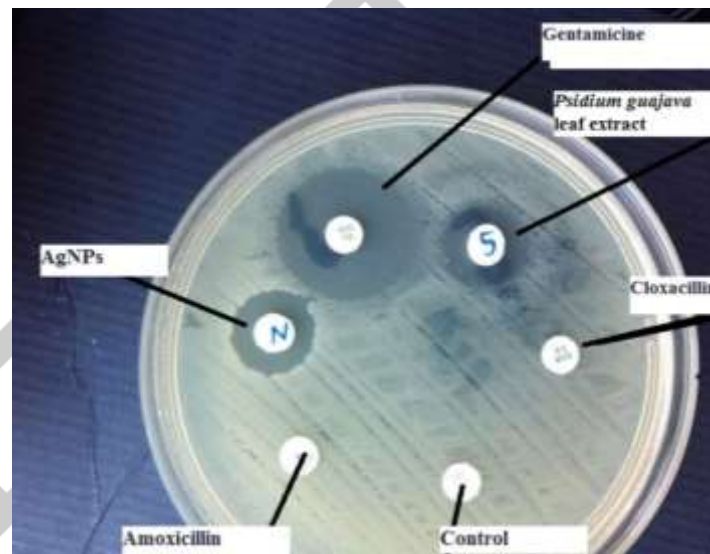
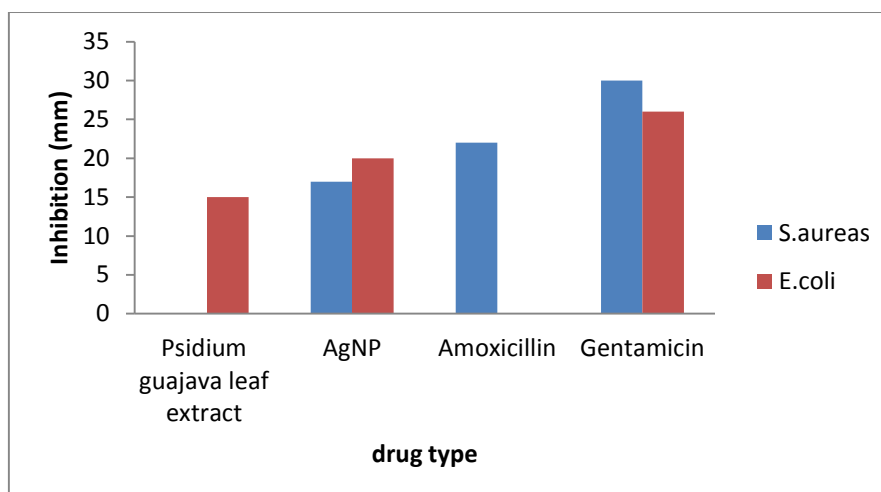


Figure 13: Inhibition zone against *E. coli* bacteria strain

According to **Figure 14**, which shows the average inhibition zones against bacteria strains with inhibition zones of 20 mm and 17 mm against *E.coli* and *S.aureus* respectively in the presence of AgNPs. Gentamicin had the highest inhibition zone of 30 mm followed by AgNPs and lastly the *Psidium guajava* leaf extract. However, amoxicillin and *Psidium guajava* leaf extract could not inhibit (*E.coli*) and *S.aureus* respectively. Inhibition by *Psidium guajava* leaf extract is attributed to the presence of phytochemicals such as triterpenoids, tannins and alkaloids which have been reported to exhibit antibacterial properties. Inhibition of bacterial strains by AgNPs is facilitated by silver's high affinity for phosphorous and sulphur which are part of the cell membranes of bacteria. The results show that silver nanoparticles can cause cell lysis or inhibit cell transduction in bacteria. The high specific surface to-volume ratio of silver nanoparticles increases their contact with microorganisms, promoting the dissolution of silver ions, thereby improving biocidal effectiveness. The synthesized AgNPs had a MIC (Minimum inhibitory concentration) value of 7 mg/ml against *E. coli* and 11 mg/ml against *S. aureus*. This could be due to their size of 20 nm thus can easily reach and contact the nuclear content of bacteria. The MIC is lower when tested against *E. coli* than when tested against *S. aureus* due to the differences on the cellular wall of each strain.





**Figure 14:** Graphical representation of average inhibition zones against bacteria strains

#### 4. Conclusion

*Psidium guajava* leaf extract was successfully used in the synthesis of AgNPs. The synthesized AgNPs were fully characterized and their antibacterial activity was evaluated. The optimum condition for the synthesis of AgNPs from *Psidium guajava* leaf extract was found to be a reaction time of 2 h at a temperature of 80 °C in the presence of 11 mM silver nitrate and 8 mL *Psidium guajava* leaf extract amount. The production of AgNPs was evidenced by UV-Vis SPR band which centered at 420 nm and SEM exhibited spherical AgNPs with a size of 20 nm. Phytochemical analysis of *Psidium guajava* leaf extract revealed the potential importance of the plant part in pharmaceutical therapy. AgNPs had an average inhibition zone of 20 mm and 17 mm against *E.coli* and *S.aureus* respectively; and MIC value of 7 mg/ml against *E. coli* and 11 mg/ml against *S. aureus*. These results show the potential of AgNPs as an antibacterial agent.

#### References

- 1 K. M. M. Abou El-Nour, A. Eftaiha, A. Al-Warthan and R. A. A. Ammar, *Arab. J. Chem.*, 2010, **3**, 135–140.
- 2 N. Makuve, *Int. J. Sci. Dev. Res. (ISSN 2455-2631)*, 2021, **6**, 30–47.
- 3 M. J. Firdhouse and P. Lalitha, *J. Nanotechnol.*, 2015, **2015**, 829526.
- 4 M. Yusuf, in *Handbook of Ecomaterials*. Springer, Cham, 2019, pp. 2343–2356.
- 5 J. Pulit-Prociak and M. Banach, *Open Chem.*, 2016, **14**, 76–91.
- 6 X.-F. Zhang, Z.-G. Liu, W. Shen and S. Gurunathan, *Int. J. Mol. Sci.*, 2016, **17**, 1534.
- 7 J. Vega-Baudrit, S. M. Gamboa, E. R. Rojas and V. V. Martinez, *Int. J. Biosens. Bioelectron.*, DOI:10.15406/ijbsbe.2019.05.00172.
- 8 J. Natsuki, *Int. J. Mater. Sci. Appl.*, 2015, **4**, 325.
- 9 I. M. Chung, I. Park, K. Seung-Hyun, M. Thiruvengadam and G. Rajakumar, *Nanoscale Res. Lett.*, 2016, **11**, 1–14.
- 10 M. Noruzi, *Bioprocess Biosyst. Eng.*, 2014, **38**, 1–14.
- 11 A. Altemimi, N. Lakhssassi, A. Baharlouei, D. G. Watson and D. A. Lightfoot, *Plants (Basel, Switzerland)*, 2017, **6**, 42.
- 12 C. Krishnaraj, E. G. Jagan, S. Rajasekar, P. Selvakumar, P. T. Kalaichelvan and N. Mohan, *Colloids Surf. B. Biointerfaces*, 2010, **76**, 50–56.
- 13 J. Y. Song, E.-Y. Kwon and B. S. Kim, *Korean J. Chem. Eng.*, 2012, **29**, 1771–1775.
- 14 Y. Wang, X. He, K. Wang, X. Zhang and W. Tan, *Colloids Surf. B. Biointerfaces*, 2009, **73**, 75–79.
- 15 S. Rajeshkumar, *Resour. Technol.*, 2016, **2**, 30–35.
- 16 G. Gnanajobitha, K. Paulkumar, M. Vanaja, S. Rajeshkumar, C. Malarkodi, G. Annadurai and C. Kannan, *J. Nanostructure Chem.*, 2013, **3**, 67.
- 17 R. Shanmugam, C. KANNAN and A. Gurusamy, *Int. J. Pharma Bio Sci.*, 2012, **3**, 502–510.
- 18 P. Magudapathy, P. Gangopadhyay, B. K. Panigrahi, K. G. M. Nair and S. Dhara, *Phys. B Condens. Matter*, 2001, **299**, 142–146.
- 19 D. S. Shenoy, J. Mathew and D. Philip, *Spectrochim. Acta Part A Mol. Biomol. Spectrosc.*, 2011, **79**, 254–262.